AGU PUBLICATIONS

JGR

Journal of Geophysical Research: Atmospheres

RESEARCH ARTICLE

10.1002/2014JD021776

Key Points:

- Perform ensemble data assimilation in WACCM using DART EAKF
- Assimilate real lower, middle, and upper atmosphere observations
- Results illustrate the importance of middle/upper atmosphere observations

Correspondence to:
N. M. Pedatella,
nickp@ucar.edu

Citation:
Pedatella, N. M., K. Raeder, J. L. Anderson, and H.-L. Liu (2014), Ensemble data assimilation in the Whole Atmosphere Community Climate Model, *J. Geophys. Res. Atmos.*, *119*, 9793–9809, doi:10.1002/2014JD021776.

Received 14 MAR 2014
Accepted 8 AUG 2014
Accepted article online 12 AUG 2014
Published online 25 AUG 2014

Ensemble data assimilation in the Whole Atmosphere Community Climate Model

N. M. Pedatella[1,2], K. Raeder[3], J. L. Anderson[3], and H.-L. Liu[1]

[1]High Altitude Observatory, National Center for Atmospheric Research, Boulder, Colorado, USA, [2]Now at COSMIC Program Office, University Corporation for Atmospheric Research, Boulder, Colorado, USA, [3]Institute for Mathematics Applied to Geosciences, National Center for Atmospheric Research, Boulder, Colorado, USA

Abstract We present results pertaining to the assimilation of real lower, middle, and upper atmosphere observations in the Whole Atmosphere Community Climate Model (WACCM) using the Data Assimilation Research Testbed (DART) ensemble adjustment Kalman filter. The ability to assimilate lower atmosphere observations of aircraft and radiosonde temperature and winds, satellite drift winds, and Constellation Observing System for Meteorology, Ionosphere, and Climate refractivity along with middle/upper atmosphere temperature observations from SABER and Aura MLS is demonstrated. The WACCM+DART data assimilation system is shown to be able to reproduce the salient features, and variability, of the troposphere present in the National Centers for Environmental Prediction/National Center for Atmospheric Research Re-Analysis. In the mesosphere, the fit of WACCM+DART to observations is found to be slightly worse when only lower atmosphere observations are assimilated compared to a control experiment that is reflective of the model climatological variability. This differs from previous results which found that assimilation of lower atmosphere observations improves the fit to mesospheric observations. This discrepancy is attributed to the fact that due to the gravity wave drag parameterizations, the model climatology differs significantly from the observations in the mesosphere, and this is not corrected by the assimilation of lower atmosphere observations. The fit of WACCM+DART to mesospheric observations is, however, significantly improved compared to the control experiment when middle/upper atmosphere observations are assimilated. We find that assimilating SABER observations reduces the root-mean-square error and bias of WACCM+DART relative to the independent Aura MLS observations by ∼50%, demonstrating that assimilation of middle/upper atmosphere observations is essential for accurate specification of the mesosphere and lower thermosphere region in WACCM+DART. Last, we demonstrate that WACCM+DART is able to follow the dynamical and chemical variability during the 2009 sudden stratosphere warming, illustrating the capability of WACCM+DART to generate high-quality atmospheric reanalysis from the surface to the lower thermosphere.

1. Introduction

Owing to the lack of comprehensive global observations in the mesosphere and lower thermosphere (MLT), numerical models are an essential tool for understanding the global-scale short-term (i.e., day-to-day) variability in the middle and upper atmosphere. Studies of short-term variability in the MLT generally fall into two categories, idealized (mechanistic) simulations and simulations that attempt to capture the true atmospheric variability. Idealized simulations have been used to study tidal variability in the MLT due to, for example, the quasi 2 day wave [*Palo et al.*, 1999] and the 6 day planetary wave [*Pedatella et al.*, 2012]. The primary advantage of idealized numerical simulations is that the dynamical changes can be isolated, allowing for a clear understanding of the source of variability. Although idealized simulations can provide considerable insight into processes that occur during actual events, the dynamical variability during any specific time period is likely to be considerably more complex. This is especially true considering the significant differences that are observed between different wave events [*Tunbridge et al.*, 2011]. To fully capture, and understand, the short-term variability in the middle and upper atmosphere for individual events, it is therefore necessary to employ methods that are able to reproduce the true variability.

Various techniques have been used to study the middle and upper atmosphere variability during specific events. The simplest approach is to nudge the model toward reanalysis fields in the lowest model levels. Such an approach has been employed in the Ground-to-topside model of Atmosphere and Ionosphere for

Aeronomy (GAIA) to study the tidal variability during the 2009 sudden stratosphere warming (SSW) [*Jin et al.*, 2012]. Nudging has also been used in the Whole Atmosphere Community Climate Model (WACCM) to investigate the dynamical variability during SSWs [*Chandran et al.*, 2013; *Sassi et al.*, 2013].

A more complex, and in principle better, approach for capturing the dynamical variability during specific events is to perform data assimilation. Several different whole atmosphere models have implemented data assimilation using the three-dimensional variational (3D-Var) method. By allowing the observations to directly influence the model, data assimilation should lead to a better specification of the atmospheric state than nudging toward reanalysis fields. 3D-Var has been used to perform data assimilation in the Canadian Middle Atmosphere Model (CMAM) [*Polavarapu et al.*, 2005], the Navy Operational Global Atmospheric Prediction System Advanced Level Physics High Altitude (NOGAPS-ALPHA) [*Hoppel et al.*, 2008], and the Whole Atmosphere Model (WAM) [*Wang et al.*, 2011]. Data assimilation has been used to study the quasi 2 day wave [*McCormack et al.*, 2009], polar mesospheric clouds [*Siskind et al.*, 2011], and SSWs [*Coy et al.*, 2009; *Ren et al.*, 2011; *Wang et al.*, 2011]. Data assimilation using 3D-Var is, however, not without potential problems. In particular, spurious correlations may occur due to incorrect specification of the background error covariance [*Polavarapu et al.*, 2005]. Furthermore, various filtering techniques are often used to prevent tidal damping, and the results at MLT altitudes are sensitive to the filtering method [*Sankey et al.*, 2007].

Ensemble data assimilation methods are an alternative approach for performing data assimilation in whole atmosphere models. In ensemble data assimilation the background error covariance is obtained directly from the ensemble members. This eliminates the need to specify the background error covariance and thus reduces the potential for spurious correlations occurring due to errors in the specified background covariance. The ensemble data assimilation is thus potentially advantageous for performing data assimilation in whole atmosphere models. *Pedatella et al.* [2013] have recently presented results based on using the Data Assimilation Research Testbed (DART) ensemble adjustment Kalman filter (EAKF) to perform data assimilation in the Whole Atmosphere Community Climate Model (WACCM). The results of *Pedatella et al.* [2013] were based on synthetic observations and for the assumption of a perfect model (i.e., no model bias or error). The results are thus limited in that they do not include any model error due to incorrect parameterizations, subgrid scale processes, model assumptions, etc. Though observation error was considered, the influence of observation noise, and potentially spurious observations, that occur in real observations were also not considered. It is therefore important to assess the performance, and potential limitations, of WACCM+DART under realistic conditions, and this is the objective of the current study. In the present study, we demonstrate the performance of WACCM+DART in the troposphere and mesosphere and illustrate the role of different observations on the results in the mesosphere. The capability of WACCM+DART to study short-term chemical and dynamical variability is also discussed based on simulations of the 2009 SSW.

2. WACCM+DART

A description of the WACCM+DART data assimilation system is provided by *Pedatella et al.* [2013]. The present study uses an identical configuration as *Pedatella et al.* [2013], and we thus only provide a brief description of the model and implementation of the data assimilation herein. WACCM is the high-top version of the National Center for Atmospheric Research (NCAR) Community Atmosphere Model (CAM). The experiments performed for the present study use a horizontal resolution of $1.9^\circ \times 2.5^\circ$ in latitude and longitude. Sixty-six vertical levels are included between the surface and the model upper boundary (5×10^{-6} hPa, $\sim$145 km). The vertical resolution varies from roughly 1.1 to 1.7 km in the troposphere and stratosphere to 3.5 km in the mesosphere and thermosphere. Details regarding the model parameterizations in WACCM can be found in *Garcia et al.* [2007], *Marsh et al.* [2007], and *Richter et al.* [2010]. The data assimilation component of WACCM+DART is provided by the DART EAKF [*Anderson*, 2001]. DART is an open-source, community, software package for performing ensemble data assimilation. The data assimilation tools provided by DART are independent of the model, and DART has been used to perform data assimilation in numerous geophysical models [*Anderson et al.*, 2009, http://www.image.ucar.edu/DAReS/DART/].

In the present study we assimilate conventional lower atmosphere observations, as well as middle/upper atmosphere temperature observations from the Sounding of the Atmosphere using Broadband Emission Radiometry (SABER) instrument on the Thermosphere Ionosphere Mesosphere Energetics Dynamics satellite and the Aura Microwave Limb Sounder (MLS). The lower atmosphere observations include aircraft and radiosonde temperature and wind observations, satellite drift winds, and Constellation Observing System for Meteorology, Ionosphere, and Climate (COSMIC) refractivity observations. Note that we currently do not assimilate satellite radiances, which are known to have a significant impact on data assimilation in the troposphere and stratosphere [e.g., *Derber and Wu*, 1998]. Though the lack of radiance assimilation is a potential shortcoming of WACCM+DART, the results presented herein demonstrate that the observation set used for the present study is sufficient to constrain the lower atmosphere. We would, however, expect to see some improvement by assimilating radiance observations. The SABER and Aura MLS temperature observations are assimilated between 100–5 $\times 10^{-4}$ hPa ($\sim$15–100 km) and 260–1 $\times 10^{-3}$ hPa ($\sim$10–95 km), respectively. Although a bias is known to exist between the SABER and Aura MLS temperature observations [e.g., *Hoppel et al.*, 2008], we do not correct for this bias since our experiments indicate that the WACCM model bias exceeds the bias between the SABER and Aura MLS observations. Correcting for the observational bias is expected to improve the results, but we have left the bias uncorrected for this report owing to the large model bias. It is important to note that the distribution of observations is significantly different in the lower atmosphere compared to the middle/upper atmosphere, and this will influence the performance of WACCM+DART at different altitudes. The lower atmosphere observations are nearly global in coverage, though they are unevenly distributed with significantly more observations over North America and Europe. In contrast, the middle/upper atmosphere observations from SABER and Aura MLS are limited to two longitudes per satellite orbit ($\sim$90 min). The SABER observations are quasi Sun synchronous, with the local time of the observations changing by $\sim$12 min d^{-1}. The Aura MLS observations are at fixed local times of 0130 and 1330 LT. The lack of comprehensive middle/upper atmosphere observations means that the data assimilation provides significantly less constraint at these altitudes relative to the troposphere and lower stratosphere. It should also be noted that the behavior of WACCM+DART in the MLT is potentially influenced by the distribution of the SABER and Aura MLS observations relative to each other, and additional studies are necessary to determine how the relative sampling may influence the results.

To demonstrate the assimilation of real observations in WACCM+DART, we have performed several experiments. First, for comparison with previous tropospheric results from CAM+DART [*Raeder et al.*, 2012], lower atmosphere observations were assimilated in WACCM+DART during the time period of 1–20 November 2008. A second set of WACCM+DART experiments was run for 9–30 September 2011 and is used to elucidate the role of the lower atmosphere observations on MLT altitudes in WACCM+DART. This simulation is also used to demonstrate the impact that even sparse middle/upper atmosphere observations can have on the assimilation results. The 9–30 September 2011 experiments assimilate either no observations (control), only lower atmosphere observations (LA), lower atmosphere and SABER observations (LA+S), or lower atmosphere, SABER, and Aura MLS observations (LA+S+A). Note that we have performed assimilations with only SABER observations in the middle atmosphere so that the results can be compared with independent Aura MLS observations. Additional WACCM+DART experiments assimilating either only lower atmosphere (LA) or our full set of observations (i.e., lower atmosphere, SABER, and Aura MLS) were performed for January and February 2009. Note that the LA experiment was only performed for days 10–50, while the LA+S+A experiment encompasses all of January and February. These experiments are used to demonstrate the capability of WACCM+DART to follow the dynamical and chemical variability during the SSW that occurred during this time period [e.g., *Manney et al.*, 2009]. For all of the WACCM+DART experiments, the assimilation is performed every 6 h; however, we only assimilate SABER and Aura MLS observations that are within $\pm$1.5 h of the assimilation time. Each experiment is performed using a 40 member ensemble. All of the September 2011 experiments are initialized from the same set of ensemble members. Similar to *Pedatella et al.* [2013], the horizontal and vertical localizations are specified with a Gaspari-Cohn function [*Gaspari and Cohn*, 1999] with half widths of 0.2 radians and 0.5 in $ln(p/p_0)$ coordinates, respectively. Spatially and temporally varying adaptive inflation is used to inflate the ensemble prior to the assimilation in order to prevent collapse of the model spread [*Anderson*, 2009].

3. Results at Tropospheric Altitudes

Prior to discussing the results in the MLT, we first present results demonstrating the performance of WACCM+DART in the troposphere. Validating the troposphere results is important since the troposphere variability has been shown to impact large-scale variability at MLT altitudes [e.g., *Liu et al.*, 2009; *Nezlin et al.*, 2009]. The 500 hPa geopotential height from the National Centers for Environmental Prediction (NCEP)/NCAR reanalysis [*Kalnay et al.*, 1996], CAM+DART [*Raeder et al.*, 2012], and WACCM+DART at 0000 UT on 15 and 19 November 2008 are shown in Figure 1. The CAM+DART and WACCM+DART results are for

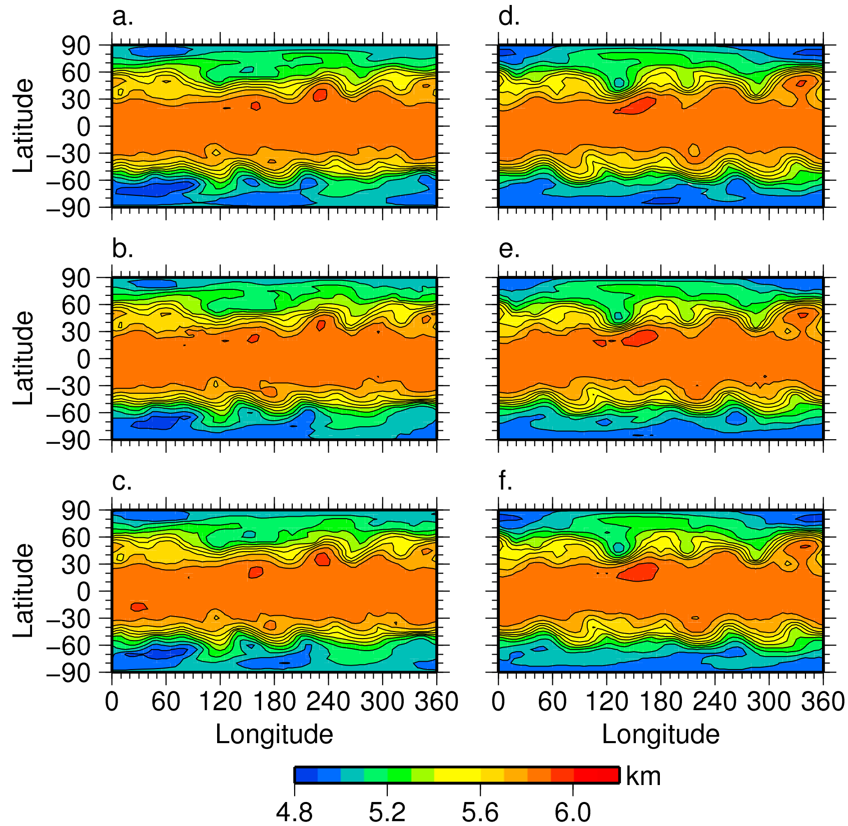

Figure 1. The 500 hPa geopotential height on 15 November 2008 at 0000 UT from (a) NCEP/NCAR reanalysis, (b) WACCM+DART, and (c) CAM+DART. (d–f) The same as Figures 1a–1c except for on 19 November 2008 at 0 UT. The CAM+DART and WACCM+DART results are for the ensemble mean.

the ensemble mean. Note that the CAM+DART results are based on an 80 member ensemble using the approach detailed in *Raeder et al.* [2012]. As seen in Figure 1, both CAM+DART and WACCM+DART reproduce the large-scale features that are present in the NCEP/NCAR reanalysis. Furthermore, the variability in the troposphere between 15 and 19 November in the NCEP/NCAR reanalysis is well captured by CAM+DART and WACCM+DART. While not an extensive validation, the results in Figure 1 illustrate that WACCM+DART can reproduce the large-scale features, and variability, of the troposphere.

As further validation of the WACCM+DART results in the troposphere, Figure 2 shows the root-mean-square error (RMSE) and bias observations minus model of WACCM+DART relative to radiosonde temperature observations averaged over North America. Note that what we refer to as bias is sometimes referred to as observation-forecast (O-F) or observation minus the analysis. In Figure 2, and throughout the following, we only present results for 20–30 September 2011 when the assimilation has reached a steady state. The 6 h forecasts are shown in Figures 2a and 2c, and the results of the analysis (i.e., model state after the assimilation) are shown in Figures 2b and 2d. As expected, the RMSE and bias of the analysis are less than the forecast results. Although there is some day-to-day variability, in the midtroposphere the 6 h forecast RMSE is ∼1 K and is closer to 1.5 K in the upper troposphere. The RMSE is thus generally similar to the results for CAM+DART [*Raeder et al.*, 2012, Figure 2], further validating the performance of WACCM+DART in the troposphere. The WACCM+DART bias relative to the radiosonde observations in the troposphere is typically less than ±0.5 K. The bias tends to be negative, indicating that the WACCM+DART temperatures are larger than the observations. The tropospheric bias in WACCM+DART is thought to be related to a general bias in tropospheric temperatures in CAM [e.g., *Neale et al.*, 2013] that is not entirely eliminated by the data assimilation. Using 3D-Var to perform data assimilation in CMAM, *Polavarapu et al.* [2005] showed forecast standard deviations of 1–2 K relative to radiosonde observations in the troposphere. The CMAM forecast bias was found to be up to 0.5 K in the troposphere. These values are similar to WACCM+DART, demonstrating that the

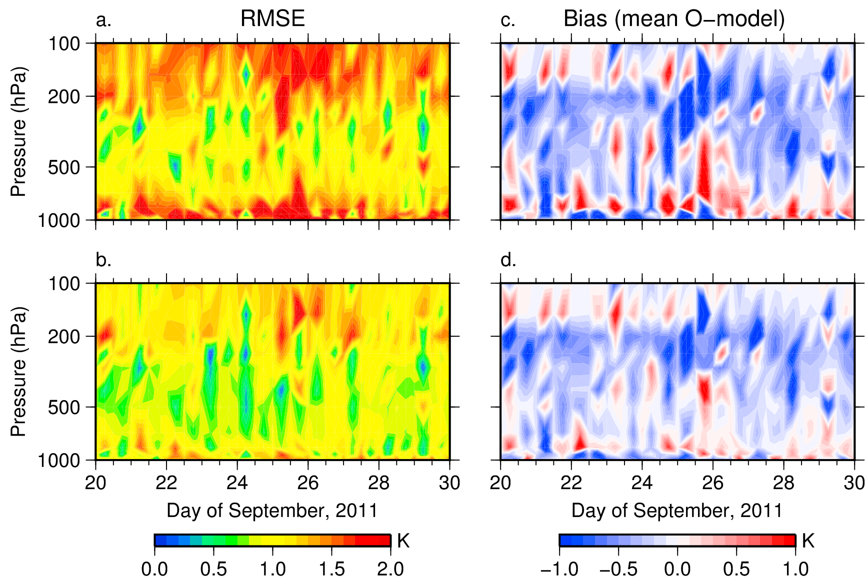

Figure 2. The root-mean-square error of the WACCM+DART (a) 6 h forecast and (b) analysis relative to radiosonde temperature observations over North America. (c, d) The same as Figures 2a and 2b except for the bias (mean O-model) of WACCM+DART relative to the observations.

performance of WACCM+DART is similar to other high-top data assimilation models despite the limited set of observations that are assimilated at lower altitudes.

4. Mesosphere and Lower Thermosphere Results

Vertical profiles of the RMSE and bias of WACCM+DART relative to SABER and Aura MLS temperature observations are shown in Figure 3. The results in Figure 3 are the global average for days 20–30 September 2011. Results are shown for the control, LA, LA+S, and LA+S+A experiments in order to show the influence of the different observations on the results. Compared to the control experiment, the assimilation of lower atmosphere observations reduces the RMSE and bias at lower altitudes. However, at higher altitudes the RMSE and bias are similar or slightly increased. This indicates that when compared to SABER and Aura MLS observations, the error of WACCM+DART in the mesosphere is nearly the same when lower atmosphere observations are assimilated compared to the climatological model variability. It is important to recognize that this indicates that the error in the control and LA experiments are statistically very similar when compared directly to the observations. It does not, however, imply that dynamical variability in the MLT is fully independent of lower atmosphere variability. We note that this result contradicts our previous study which found that assimilating lower atmosphere observations reduced the global average RMSE by ∼40% in the MLT [*Pedatella et al.*, 2013]. It is important to note that our previous study used synthetic observations that were sampled from a known model truth, and the results thus assume that there is no model bias or error due to inaccurate model parameterizations, subgrid-scale processes, etc. Furthermore, in our previous study the RMSE was calculated with respect to the known model state, and not compared directly to the synthetic observations. For a more direct comparison with the present results, Figures 3e and 3f show the RMSE and bias with respect to the synthetic SABER observations from the experiments of *Pedatella et al.* [2013]. Figures 3e and 3f clearly show that under the assumption of a perfect model, the assimilation of lower atmosphere observations improves the fit of WACCM+DART to SABER observations compared to the control experiment that does not assimilate any observations. This leads to the conclusion that at least for the present version of WACCM, constraint of the lower atmosphere through data assimilation improves the fit of WACCM+DART to observations in the MLT for the perfect model case but not for the case of assimilating real observations. We again emphasize that this conclusion is strictly with regards to comparison of the model state directly to the observations, and it does not necessarily imply that constraining the lower atmosphere has no impact on the mesosphere. As discussed below, future improvements in WACCM will potentially make this conclusion invalid, resulting in improved specification of the MLT in WACCM+DART when lower atmosphere observations are assimilated.

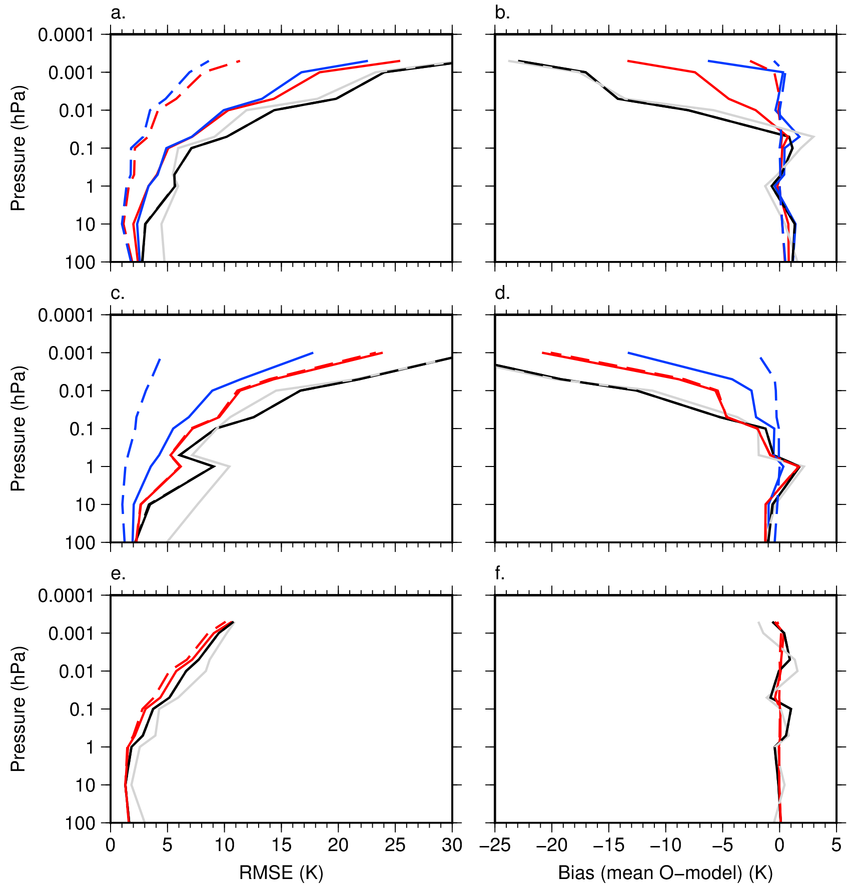

Figure 3. The global average (a) root-mean-square error and (b) bias (mean O-model) of WACCM+DART relative to SABER observations for the control (grey), LA (black), LA+S (red), and LA+S+A (blue) experiments. (c, d) The same as Figures 3a and 3b except for Aura MLS observations. (e, f) The same as Figures 3a and 3b except that the results are for experiments using synthetic observations. Solid and dashed lines are for the 6 h forecast and analysis, respectively.

Gravity wave drag is known to be a key mechanism for establishing the mean circulation and temperature of the mesosphere [*Alexander et al.*, 2010] and also for coupling between variability in the lower atmosphere and the mesosphere [e.g., *McLandress et al.*, 2013]. We therefore believe that the lack of impact of real lower atmosphere observations on WACCM+DART relative to mesospheric observations is likely to be related to the gravity wave drag parameterization in WACCM. As will be discussed in more detail below, the WACCM climatology is known to be biased in the mesosphere, and this is largely related to the gravity wave drag parameterization. The large climatological bias is clearly evident in Figure 3, and assimilating only lower atmosphere observations does not significantly impact this bias. We therefore believe that the RMSE and bias with respect to mesospheric observations are dominated by inaccurate model climatology, which is due to deficiencies in the gravity wave drag parameterization. That is, the RMSE and bias in the LA experiment are primarily influenced by errors in the MLT thermal structure and general circulation, which are in turn determined by unresolved gravity waves. Though assimilating lower atmosphere observations will impact large-scale waves, such as planetary waves and tides, the lower atmosphere observations do not directly influence the MLT thermal structure and general circulation, and this results in the impact of lower atmosphere observations in the MLT being overwhelmed by errors in the model climatology. Future improvements in the WACCM climatology would reduce the influence of errors in the model climatology on the RMSE and bias. The RMSE and bias would then be more influenced by variations on spatial and temporal scales that are impacted by the lower atmosphere observations, and we hypothesize that this would lead to an improved fit of WACCM+DART to observations in the mesosphere when lower atmosphere observations are assimilated. It is important to note that any potential deficiencies in the current gravity wave drag scheme does not prevent reliable estimates of the middle atmosphere state in WACCM+DART. As discussed later, the RMSE and bias in the mesosphere are drastically reduced when SABER and Aura MLS

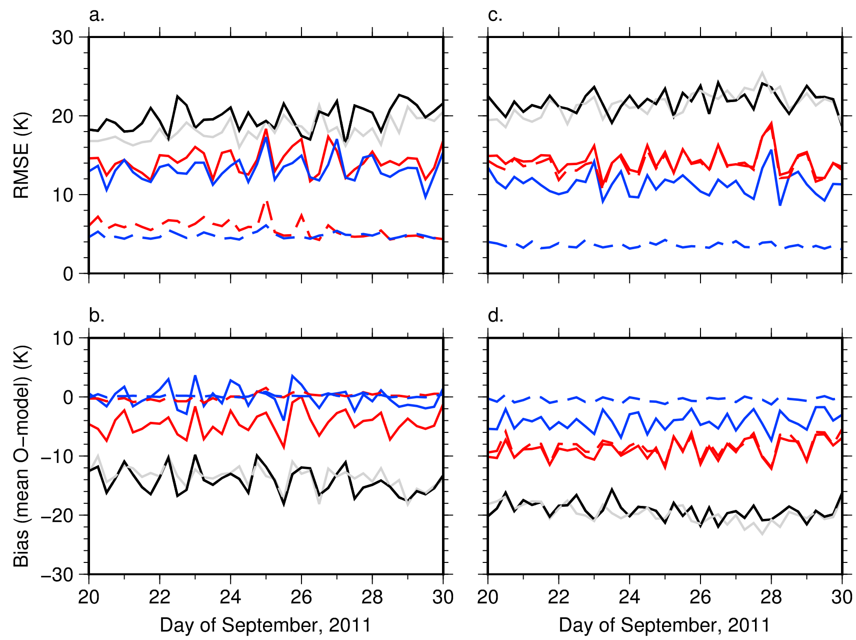

Figure 4. The global average (a) root-mean-square error and (b) bias (mean O-model) of WACCM+DART relative to SABER observations at 5×10^{-3} hPa for the control (grey), LA (black), LA+S (red), and LA+S+A (blue) experiments. (c, d) The same as Figures 4a and 4b except for Aura MLS observations. Solid and dashed lines are for the 6 h forecast and analysis, respectively. Note that the RMSE and bias are plotted using different vertical axes.

observations are assimilated, and it is therefore possible to accurately specify the middle atmosphere state in WACCM+DART. We further note that the errors relative to SABER observations in the WACCM+DART LA experiment are similar to those in other whole atmosphere data assimilation models. Any deficiencies in the gravity wave drag parameterization thus do not introduce exceedingly large errors, at least in comparison to schemes employed in other models. For example, comparison of the present results with those of CMAM [*Ren et al.*, 2011] and the Navy Global Environmental Model (NAVGEM, a follow-on to NOGAPS-ALPHA) [*Hoppel et al.*, 2013] illustrates similar 6 h forecast errors relative to SABER observations in all three models when only lower atmosphere observations are assimilated. This indicates that despite shortcomings in the gravity wave drag parameterization, the impact of lower atmosphere observations on the mesosphere in WACCM+DART is similar to other middle atmosphere data assimilation models. The statistical similarity between the control and LA experiments when compared directly to observations may therefore not be unique to WACCM+DART, though this will depend on the amount of internal model variability.

Although the assimilation of lower atmosphere observations does not improve the fit of WACCM+DART to mesosphere observations, the assimilation of SABER and Aura MLS temperature observations leads to a significant improvement in the RMSE and bias relative to the control experiment. In particular, as seen in Figures 3c and 3d, the assimilation of SABER observations reduces the 6 h forecast RMSE and bias of WACCM+DART with respect to Aura MLS observations. This demonstrates that assimilating SABER observations significantly improves the assimilation results in the middle/upper atmosphere when compared to an independent set of observations. Furthermore, the fact that the 6 h forecast and analysis are similar (the analysis is not clearly apparent in Figures 3c and 3d due to the similarity of the forecast and analysis) indicates that the assimilation of the SABER observations is not directly impacting the locations of the Aura MLS observations. Rather, the improvement in the fit to Aura MLS observations comes from an overall improvement in the specification of the middle/upper atmospheric state when the SABER observations are assimilated. When assimilating SABER and Aura MLS observations, the forecast RMSE is 8–9 K at 0.01 hPa and 5–6 K at 0.1 hPa for both SABER and Aura MLS. Results of NAVGEM are similar [*Hoppel et al.*, 2013], again illustrating that WACCM+DART performs similar to other middle atmosphere data assimilation models.

The impact of the SABER and Aura MLS observations on the assimilation results in the MLT can be seen more clearly in Figure 4, which shows the RMSE and bias at 5×10^{-3} hPa (~85 km) of WACCM+DART relative to SABER and Aura MLS observations in the Northern Hemisphere. When only assimilating lower atmosphere

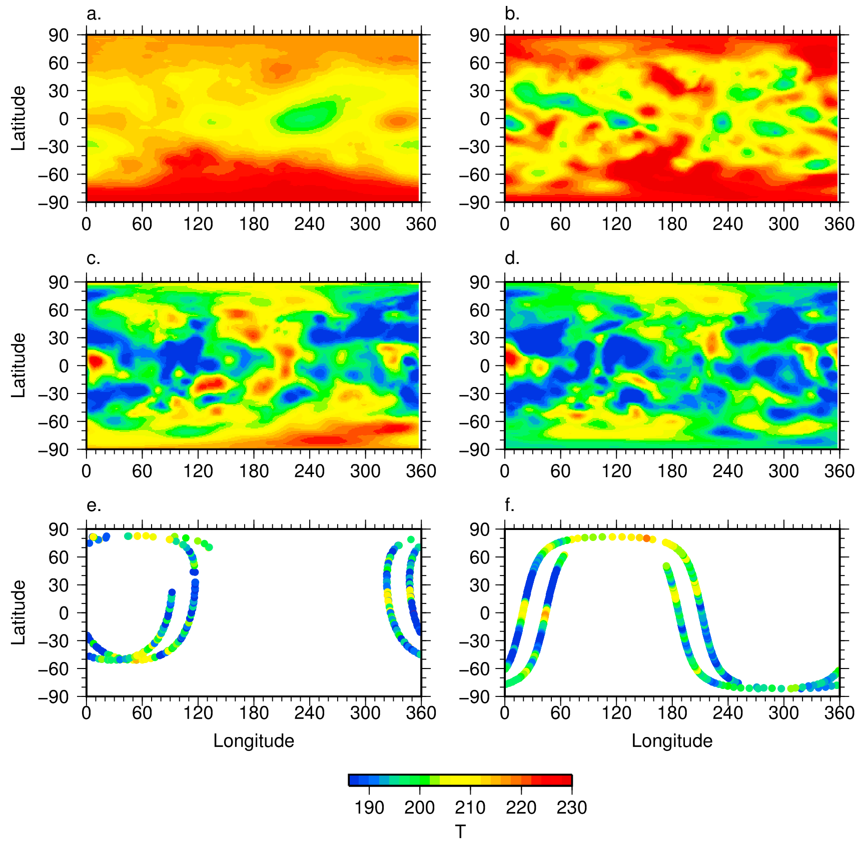

Figure 5. WACCM+DART temperature at 5×10^{-3} hPa on 29 September 2011 at 0000 UT for (a) control, (b) LA, (c) LA+S, and (d) LA+S+A experiments. (e) SABER and (f) Aura MLS observations that were assimilated in WACCM+DART.

observations, the RMSE of WACCM+DART with respect to both SABER and Aura MLS temperature observations is ~20 K, which is 1–2 K larger than the control experiment. The additional assimilation of SABER observations reduces the RMSE of the 6 h forecast by 50% to around 10 K for both the SABER and Aura MLS observations. The analysis RMSE is ~5 K with respect to SABER observations for this case, while the 6 h forecast and analysis RMSE are again similar for the Aura MLS observations indicating that the SABER observations are not directly impacting the locations of the Aura MLS observations. The 6 h forecast RMSE and bias with respect to both SABER and Aura MLS observations for the LA+S+A case are 1–2 K (~10%) less than the LA+S case. This is an important result, and it demonstrates that the assimilation of the Aura MLS observations can improve the fit of the 6 h WACCM+DART forecast for both the SABER and Aura MLS observations. The additional improvement that comes from assimilating the Aura MLS observations occurs primarily in the Southern Hemisphere, which was not observed by SABER during 20–30 September 2011. Though they still lead to an improvement in the RMSE and bias, the impact of the Aura MLS observations is considerably less in the Northern Hemisphere.

From Figures 4b and 4d it is apparent that there is a significant bias between the observed and modeled temperatures in the MLT. This confirms that the bias between SABER and Aura MLS observations is negligible compared to the model bias in this case. The model bias is not surprising since WACCM is known to have a warm bias in the mesosphere [e.g., *Garcia et al.*, 2007; *Yuan et al.*, 2008; *Marsh et al.*, 2013a], and there is an ongoing effort to remove this bias. To more clearly illustrate the bias and the influence of the data assimilation on correcting the bias, the WACCM+DART temperature at 5×10^{-3} hPa at 0000 UT on 29 September 2011 is shown in Figure 5. Results are shown for the control, LA, LA+S, and LA+S+A experiments, along with the SABER and Aura MLS observations that are within the assimilation window. The large bias in mesospheric temperature between the control and LA experiments and the observations is clearly evident in Figure 5, especially at high latitudes. Furthermore, the results in Figure 5 demonstrate that the assimilation of SABER observations reduces the bias globally, and not only in the location of the observations. For

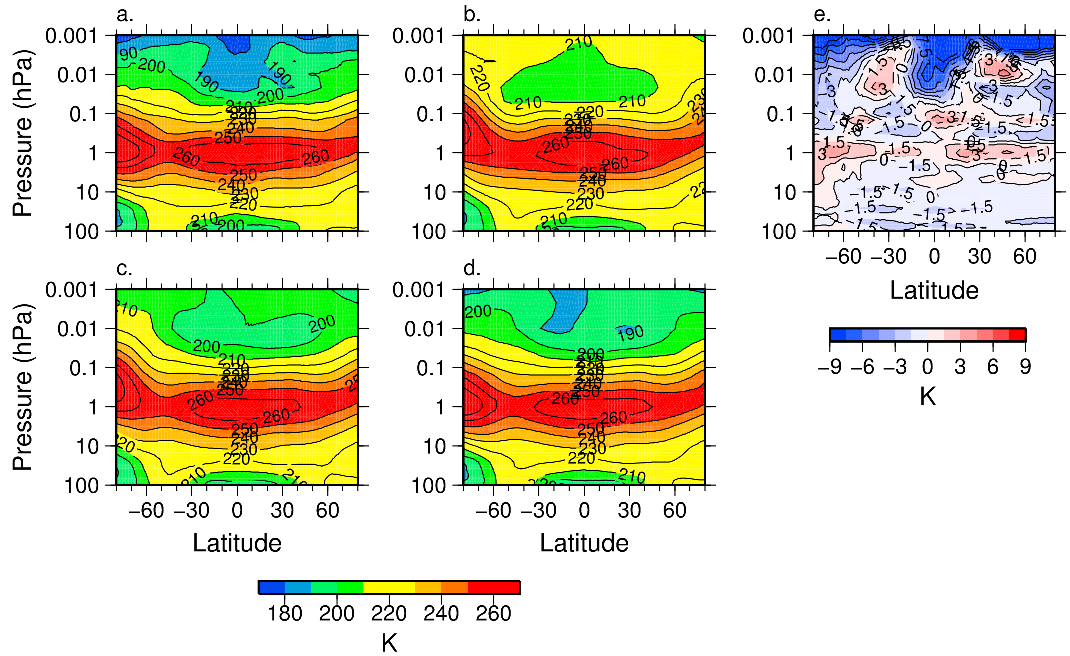

Figure 6. The zonal mean temperature averaged between 20 and 30 September 2011 near 1400 LT from (a) Aura MLS observations and the (b) LA, (c) LA+S, and (d) LA+S+A WACCM+DART experiments. (e) The difference between Figures 6a and 6d.

example, despite the fact that there are no SABER observations in this region, the temperature is reduced at high latitudes in the Southern Hemisphere in the LA+S experiment. The additional assimilation of Aura MLS observations further reduces the global temperature bias, and it is again apparent that this occurs not only in regions that are directly influenced by the observations at this assimilation epoch. The results in Figure 5 thus demonstrate that even relatively sparse observations in the middle/upper atmosphere have a global impact on the state of the mesosphere.

To further illustrate the impact of data assimilation on reducing the WACCM temperature bias, the zonal mean temperature averaged from 20 to 30 September near 1400 local time is shown in Figure 6 for the Aura MLS observations and the LA, LA+S, and LA+S+A WACCM+DART assimilation results. The difference (observations minus model) between the Aura MLS observations and LA+S+A WACCM+DART results are shown in Figure 6e. The results in Figure 6a are based on the mean of the Aura MLS observations in 2° latitude bins at each height for the ascending portion of the Aura orbit. Note that for altitudes above 0.01 hPa, the Aura MLS observations are potentially biased by up to −9 K [e.g., *Schwartz et al.*, 2008], and the comparison in Figure 6 should be considered in the context of this temperature bias. The Aura MLS observations are consistent with the WACCM+DART results in the stratosphere. However, the observations reveal a slightly warmer stratopause and a significantly cooler mesosphere compared to the LA experiment. For the LA experiment, WACCM+DART is 10–20 K warmer than the observations in the mesosphere. Given the previously mentioned mesospheric bias in WACCM, we anticipate the large bias between the Aura MLS observations and WACCM+DART when only lower atmosphere observations are assimilated. The assimilation of SABER temperature observations reduces the model bias to roughly −10 K in the mesosphere, resulting in a significantly improved representation of mesospheric temperatures. Though no longer a comparison with independent observations, the addition of the Aura MLS observations further reduces the model warm bias in the mesosphere. As seen in Figure 6e, the difference between the Aura MLS and LA+S+A WACCM+DART zonal mean temperature is generally less than 1–2 K up to 0.01 hPa, which is similar to results for NOGAPS-ALPHA [*Eckermann et al.*, 2009]. Above 0.005 hPa, the bias grows significantly; however, as noted above, this can be partly attributed to the large bias of Aura MLS at these altitudes. The overall reduction in the model bias is significant and demonstrates that the atmospheric state in the stratosphere and mesosphere in WACCM+DART can be significantly improved by assimilating middle/upper atmosphere observations. *Ren et al.* [2011] and *Hoppel et al.* [2013] also found that a significant reduction in mesosphere temperature bias occurred when middle/upper atmosphere observations were assimilated

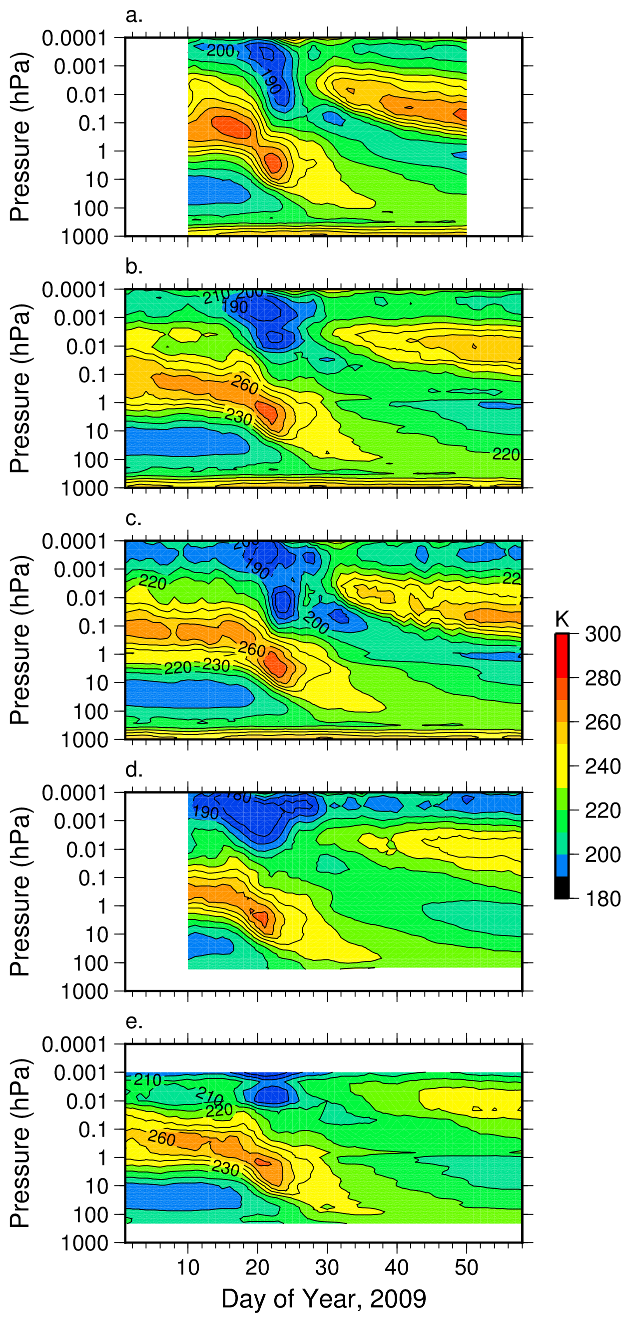

Figure 7. Zonal mean temperature averaged between 70 and 90°N for (a) WACCM+DART LA, (b) LA+S+A, (c) SD-WACCM, (d) SABER, and (e) Aura MLS. Note that the Aura MLS observations are averaged between 70 and 80°N. SABER did not sample high latitudes in the Northern Hemisphere prior to day 11.

compared to only assimilating lower atmosphere observations. The importance of middle/upper atmosphere observations on accurately modeling MLT altitudes is thus not unique to WACCM+DART.

5. The 2009 Sudden Stratosphere Warming

WACCM+DART experiments for January and February 2009 were performed in order to demonstrate that WACCM+DART can create a high-quality reanalysis from the surface to the lower thermosphere. Such reanalyses are extremely useful for studying the chemical and dynamical processes during events such as SSWs. We focus on the 2009 SSW since it is well documented observationally [*Funke et al.*, 2010; *Manney et al.*, 2009]. Furthermore, several high top, and whole atmosphere models, have simulated this event [*McLandress et al.*, 2013; *Pedatella et al.*, 2014], permitting a comparison of WACCM+DART to both observations and other model simulations. Figure 7 shows the zonal mean temperature averaged from 70 to 90°N for January and February 2009 from the WACCM+DART LA and LA+S+A experiments, specified dynamics WACCM (SD-WACCM), SABER, and Aura MLS observations. Note that Aura MLS does not observe poleward of 80°N, and the Aura MLS results are thus averaged between 70 and 80°N. The SD-WACCM results are from simulations performed by *Marsh et al.* [2013b], and in these simulations, WACCM is constrained through nudging the model dynamical fields toward reanalysis from the NASA Modern-Era Retrospective Analysis for Research and Applications (MERRA) up to 50 km. Nudging toward reanalysis, as done in SD-WACCM, is the method typically employed to reproduce the atmospheric state in WACCM during specific time intervals. The present comparison thus provides a sense of the performance of WACCM+DART relative to the method that is currently used in WACCM. It can be seen in Figure 7 that the salient features of the SSW are reproduced in the WACCM+DART (Figures 7a and 7b) and SD-WACCM (Figure 7c) simulations. For example, all of the simulations reproduce the stratopause descent and subsequent warming of the stratosphere, beginning around days 18–20. A strong mesospheric cooling is also present between roughly days 15–30. Beginning around day 30, elevated stratopause forms near ∼0.005 hPa in the simulations. The stratopause descent, mesospheric cooling, an elevated

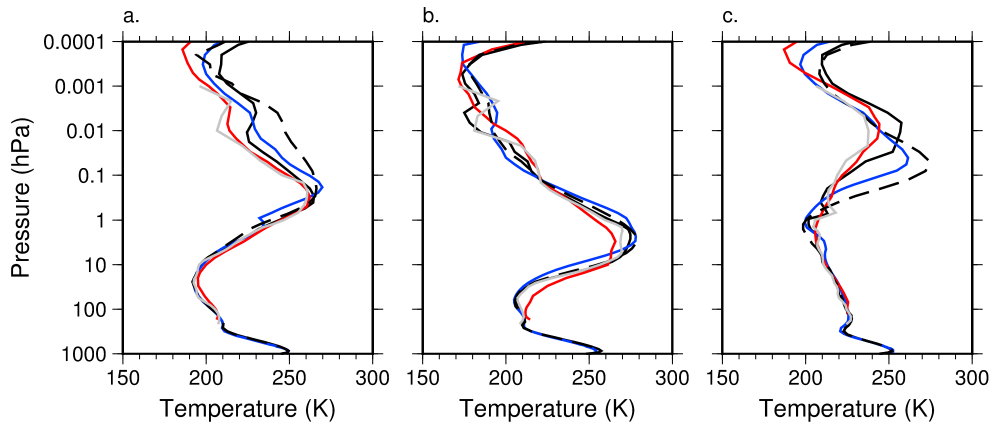

Figure 8. Zonal mean temperature averaged between 70 and 90°N for WACCM+DART LA (dashed black), LA+S+A (solid black), SD-WACCM (blue), SABER (red), and Aura MLS (grey) on day of year (a) 12, (b) 24, and (c) 50 in 2009.

stratopause simulated by WACCM+DART and SD-WACCM are generally consistent with the SABER and Aura MLS observations.

The results of the WACCM+DART LA experiment during 2009 may, at first, appear to contradict the results in the previous section, since it is clear that assimilation of the lower atmosphere observations influences the mesosphere. However, we again emphasize that the prior comparison was strictly a statistical comparison of WACCM+DART relative to observations and did not imply that the lower atmosphere does not drive variability in the mesosphere. Figure 7a demonstrates that assimilation of observations in the lower atmosphere does impact the state of the mesosphere in WACCM+DART. This is consistent with prior studies on the impact of the lower atmosphere on middle/upper atmosphere variability [e.g., *Ren et al.*, 2011; *McLandress et al.*, 2013]. Though the lower atmosphere observations do impact the mesosphere during the 2009 SSW, the WACCM+DART LA and SD-WACCM simulations remain biased relative to the observations, though this is less apparent due to the dramatic changes that occur in the MLT during the SSW. This demonstrates that the climatological errors in WACCM still impact the MLT thermal structure and dynamics during strong dynamical events and that they are potentially less noticeable due to the drastic changes that occur during these time periods.

Though many aspects of the zonal mean temperature variability in the WACCM+DART LA and LA+S+A experiments and SD-WACCM simulations are similar, there are some distinct differences. In particular, the mesopause is slightly warmer in the WACCM+DART experiments compared to SD-WACCM. There are also notable differences in the rate of descent of the elevated stratopause during February. In the WACCM+DART LA+S+A experiment, the stratopause remains near 0.01 hPa until the end of February. In contrast, the elevated stratopause in both the WACCM+DART LA and SD-WACCM experiments descends quickly, reaching nearly 0.1 hPa by the end of February. To more clearly show the similarities and differences between the simulations and the observations, vertical profiles of the zonal mean temperature averaged between 70 ad 90°N on days 12, 24, and 50 are shown in Figure 8. Prior to the SSW (Figure 8a), there is extremely good agreement between the simulations and the observations up to ~1 hPa. Here the simulations and observations begin to diverge. The stratopause in the WACCM+DART LA (dashed black) and SD-WACCM (blue) simulations are seen to be slightly higher than the observations. The height of the stratopause on this day is well captured by the WACCM+DART LA+S+A (solid black) experiment. Larger differences are apparent in the mesosphere, with the WACCM+DART LA simulation tending to be significantly too warm up to ~0.01 hPa. The WACCM+DART LA+S+A and SD-WACCM are also slightly warm compared to the observations in the mesosphere. Though there are some slight differences, at all altitudes, there is an overall good agreement between the three simulations and the observations on day 24. On day 50, the observations and model simulations are all in good agreement up to ~0.5 hPa. Large differences are apparent above this altitude, and the notably different altitudes of the elevated stratopause is clearly seen in Figure 8c. The WACCM+DART LA+S+A stratopause height is in good agreement with the observations. It is, however, warmer than the SABER and Aura MLS observations. The stratopause in WACCM+DART LA and SD-WACCM is also warmer than the observations, and it is seen to be at a significantly lower altitude.

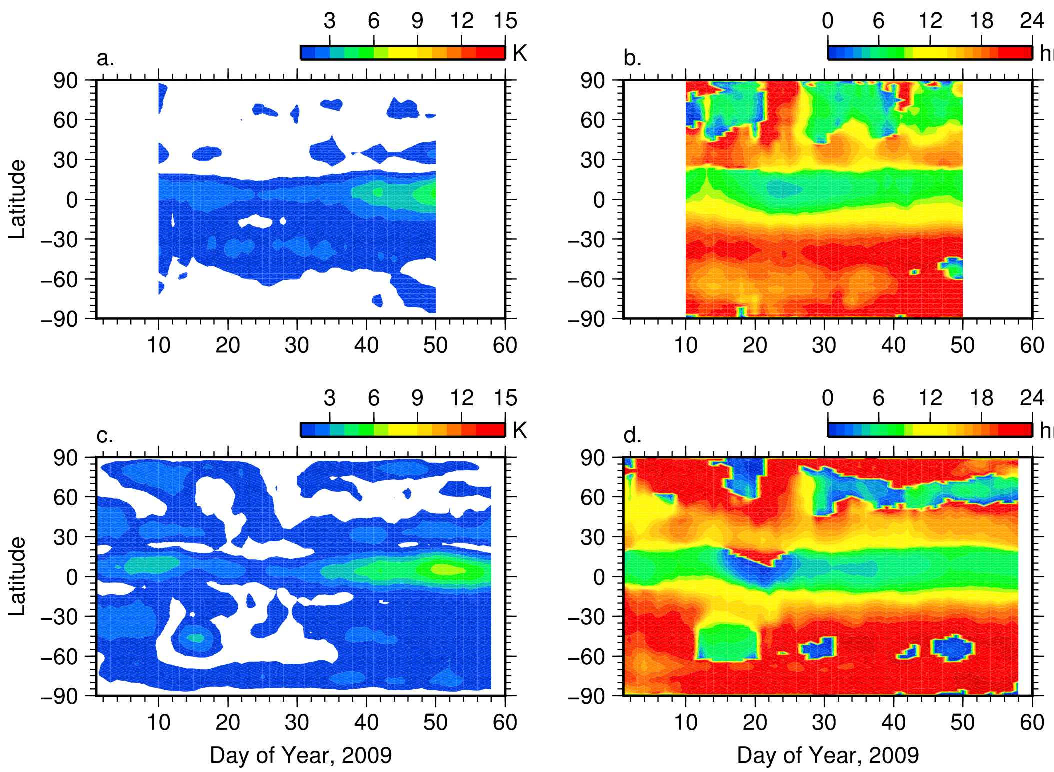

Figure 9. WACCM+DART DW1 (a) amplitude and (b) phase at 0.01 hPa for the 2009 LA experiment. (c, d) Same as Figures 9a and 9b except for 2009 LA+S+A experiment.

The results in Figures 7 and 8 illustrate the importance of assimilating middle and upper atmosphere observations for dynamical events such as the 2009 SSW. In particular, it is clear that the SABER and Aura MLS observations are essential for capturing features such as the elevated stratopause, which is important in terms of its influence on chemical transport [e.g., *Randall et al.*, 2009]. At least in this aspect, assimilating all observations in WACCM+DART leads to a notable improvement relative to the current approach of SD-WACCM for producing atmospheric reanalysis up to the lower thermosphere. It is worthwhile to also compare the performance of the WACCM+DART LA+S+A experiment during the 2009 SSW relative to other model simulations. Using a version of CMAM constrained in the lower atmosphere by European Centre for Medium-Range Weather Forecasts reanalysis, *McLandress et al.* [2013] presented results for the 2009 SSW. Similar to SD-WACCM and the WACCM+DART LA experiment, the elevated stratopause in CMAM appears to descend faster compared to the observations, though this may partly be related to the fact that the stratopause formed near the altitude of the upper boundary sponge layer in CMAM. *Pedatella et al.* [2014] compared the zonal mean and tidal variability during the 2009 SSW in four different whole atmosphere models, GAIA, the Hamburg Model of the Neutral and Ionized Atmosphere (HAMMONIA), WAM, and the extended version of WACCM (WACCM-X). The only model that was able to reproduce the extended duration of the stratopause at high altitudes was WACCM-X, which was nudged by a combination of NOGAPS-ALPHA and MERRA reanalyses. The elevated stratopause descended faster than observed in the GAIA and Hamburg Model of the Neutral and Ionized Atmosphere (HAMMONIA) models, and no clear elevated stratopause was seen in WAM simulations [*Pedatella et al.*, 2014, Figure 1]. Interestingly, WACCM-X constrained by NOGAPS-ALPHA/MERRA is the only other model that well reproduced the elevated stratopause and is also the only model to be influenced by middle/upper atmosphere observations, which are assimilated in NOGAPS-ALPHA. This again illustrates the importance of assimilating middle/upper atmosphere observations during events such as the 2009 SSW.

The WACCM+DART-simulated variability in the migrating diurnal (DW1) and semidiurnal (SW2) tides during the 2009 SSW are shown in Figures 9 and 10, respectively. Both the LA (top) and LA+S+A (bottom) are shown so that the influence of assimilating the Aura MLS and SABER observations on the tidal variability can be assessed. The results are shown at 0.01 hPa for the DW1 and 1×10^{-4} hPa for the SW2. Note that the

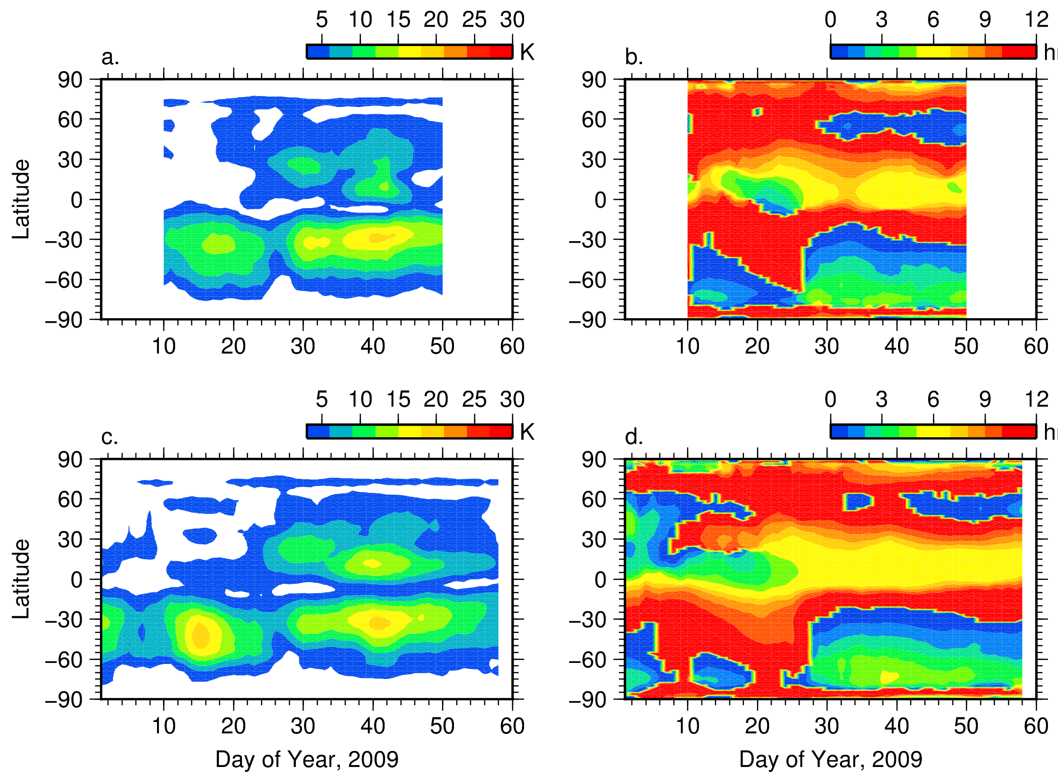

Figure 10. Same as Figure 9, except for the SW2 at 1×10^{-4} hPa.

pressure levels were chosen so that the results in Figures 9 and 10 can be directly compared with Figures 9 and 10 in *Pedatella et al.* [2014], which show the tidal variability during the 2009 SSW simulated by the GAIA, HAMMONIA, WAM, and WACCM-X models. The results for the LA and LA+S+A experiments are generally similar, although the tides are slightly stronger when the Aura MLS and SABER observations are assimilated. The similarity in the tides is partly to be expected since they originate in the lower atmosphere, and the differences in the zonal mean atmosphere are not very large, at least relative to the large-scale dynamical changes that occur during the SSW. In the equatorial region, the DW1 amplitude is decreased between days 15–35, and the phase is shifted earlier by ~6 h around days 15–30. The evolution of the DW1 amplitude and phase in WACCM+DART is similar to other whole atmosphere model simulations of the 2009 SSW [*Pedatella et al.*, 2014]. SW2 maxima of ~20–25 K occur at midlatitudes near days 15 and 40. Relative to other simulations, the SW2 in WACCM+DART is slightly weaker. This is likely related to the fact that the SW2 amplitude is generally too small in WACCM [e.g., *Davis et al.*, 2013]. The timing of the SW2 maxima is also slightly different compared to other model simulations. The maximum on day 40 in WACCM+DART occurs several days later compared to other model simulations which show maxima around days 30–35. *Sathishkumar and Sridharan* [2013] observed semidiurnal tide maxima on days 35 and 44 in zonal and meridional wind, respectively, over Tirunelveli (8.7°N, 77.8°W). Though the observations contain a mixture of tidal components, they illustrate that the exact timing of the SW2 enhancement following the SSW is uncertain. We also note that the SW2 maximizes near day 40 in WACCM-X nudged by NOGAPS-ALPHA/MERRA. The later enhancement in the SW2 in WACCM+DART and WACCM-X nudged by NOGAPS-ALPHA/MERRA may be related to the fact that the zonal mean atmospheric state is similar in these two simulations, particularly in terms of the elevated stratopause, and this may influence the temporal variability of SW2 by impacting its propagation into the MLT.

WACCM includes a comprehensive treatment of chemical processes, and WACCM+DART can thus be used to study the variability of chemical species during events such as the 2009 SSW. As an example, the WACCM+DART LA and LA+S+A zonal mean ozone variability at 2 hPa during January and February 2009 are shown in Figures 11a and 11b, respectively. The zonal mean ozone observed by SABER is shown in Figure 11c. The differences (observation minus model) are shown in Figures 11d and 11e. To prevent the

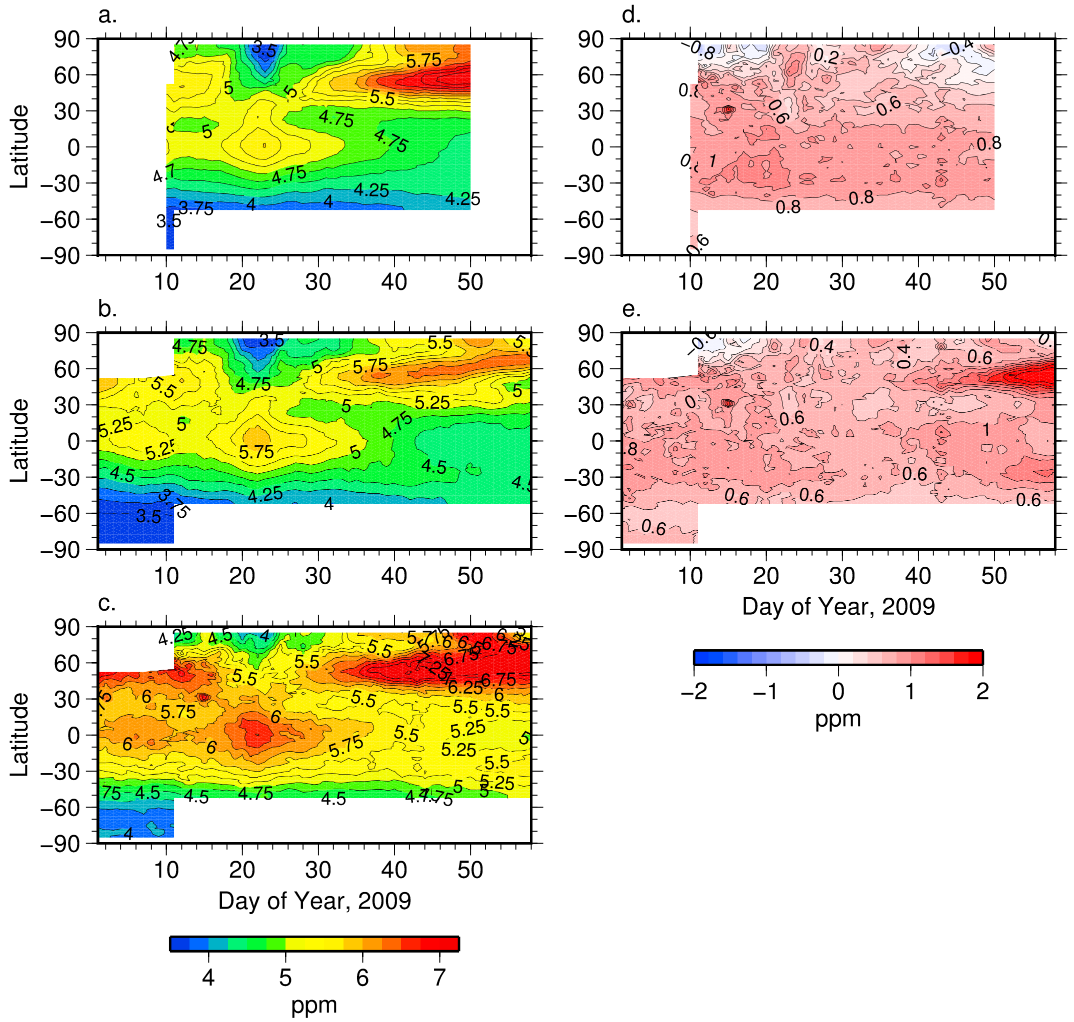

Figure 11. Zonal mean ozone at 2 hPa for the WACCM+DART (a) LA, (b) LA+S experiments, and (c) SABER observations. (d) Difference between SABER observations and WACCM+DART LA experiment. (e) Same as Figure 11d except for the LA+S experiment. Note that SABER did not observe high latitudes in the Northern Hemisphere prior to day 11 and did not observe high latitudes in the Southern Hemisphere after day 11.

limited local time sampling of the SABER observations from influencing the comparison, the WACCM+DART ozone was sampled based on the locations of the SABER observations. Ozone variability may contribute to the SW2 variability during the SSW, and it is considered to be potentially important for coupling stratospheric and ionospheric variability [e.g., *Goncharenko et al.*, 2012]. It is therefore important to accurately simulate the ozone variability during the SSW. The results in Figure 11 show an overall agreement between both WACCM+DART experiments and the SABER observations in terms of the ozone temporal variability. We attribute the similarity of the two WACCM+DART experiments to the fact that 2 hPa is not significantly above the maximum altitude of the lower atmosphere observations (~1 hPa). Around the time of the SSW, an equatorial ozone enhancement of ~1 ppm and a significant ozone depletion at high latitudes in the Northern Hemisphere can be seen in both the SABER observations and WACCM+DART. Both also show a narrow region of enhanced ozone near 60°N beginning on day 30. Since we do not directly assimilate ozone in WACCM+DART, the agreement between the WACCM+DART and SABER ozone provides an indirect validation of the WACCM+DART data assimilation system during the 2009 SSW. Though the WACCM+DART ozone agrees with the SABER observations in terms of the temporal and latitudinal variability, the SABER observations are consistently larger than the WACCM+DART values (Figures 11d and 11e). At low and middle latitudes, the WACCM+DART ozone bias is roughly 0.8–1.0 ppm for the LA experiment and 0.5–0.75 ppm for the LA+S+A experiment. Ozone variability in the upper stratosphere during SSWs is dominated by temperature changes which impact the ozone photochemistry [e.g., *Randall*, 1993], and we therefore consider the slight ozone bias between the two WACCM+DART experiments to be related to small temperature differences in these experiments. We further note that although the gross features are captured, the ozone enhancement in the Northern Hemisphere beginning around day 30 is different in the two simulations. At least up to day 50, this feature is well captured in the LA experiment. However, it is slightly weaker and narrower in the LA+S+A experiment. Based on Figure 11, we may conclude that WACCM+DART generally reproduces the ozone variability during the 2009 SSW, with the exception of a nearly constant bias between the model and observations. The constant offset between the WACCM+DART and SABER ozone is reflective of a bias in either the model or observations. *Rong et al.* [2009] found an overall high bias in SABER ozone observations in the upper stratosphere and mesosphere, and we thus attribute the general discrepancy between the SABER and WACCM+DART ozone to be due to a bias in the SABER observations. Given the known bias in the SABER ozone, the agreement in Figure 11 is considered to be good, illustrating that WACCM+DART can also be applied to understand variability in chemical species.

6. Conclusions

The present study demonstrates the ability of the WACCM+DART data assimilation system to assimilate real lower, middle, and upper atmosphere observations. In the troposphere, WACCM+DART is able to reproduce the large-scale features, and variability, that are present in the NCEP/NCAR reanalysis and CAM+DART. In the upper stratosphere and mesosphere, we find that the assimilation of only lower atmosphere observations slightly degrades the fit of WACCM+DART to SABER and Aura MLS observations compared to an experiment without any data assimilation. This indicates that the lower atmosphere observations do not improve the error in the mesosphere when comparing directly to observations. However, we emphasize that it does not necessarily imply that the lower atmosphere does not drive mesospheric variability. We hypothesize that the lack of impact of the lower atmosphere observations on the WACCM+DART fit to observations is related to the tuning of gravity wave drag parameterizations based on climatology, which may not be suitable for the data assimilation application. This demonstrates the importance of the gravity wave drag parameterizations. The assimilation of middle/upper atmosphere observations does, however, significantly improve the WACCM+DART results in the MLT. Compared to independent observations, the assimilation of middle/upper atmosphere observations reduces the RMSE and bias of WACCM+DART by ~50%. Assimilating middle/upper atmosphere observations is therefore critical for accurate specification of the middle and upper atmospheric state in WACCM+DART.

When middle/upper atmosphere observations are assimilated, WACCM+DART is found to be able to well reproduce the state of the middle atmosphere. The RMSE of WACCM+DART relative to SABER and Aura MLS observations is found to be 5–10 K at altitudes of 0.1–0.01 hPa, and the performance of WACCM+DART is thus similar to other middle atmosphere data assimilation models. Simulations of the 2009 SSW illustrate that WACCM+DART is able to reproduce the chemical and dynamical variability during SSWs. When assimilating middle/upper atmosphere observations, WACCM+DART is able to capture the extended duration of the elevated stratopause after the 2009 SSW, which is an aspect of the dynamical variability that is not well reproduced in other model simulations such as SD-WACCM. This illustrates the potential advantages of the data assimilation approach compared to nudging the model toward reanalysis fields. We further demonstrate that the short-term variability during January and February 2009 in the DW1 and SW2 tides is consistent with other model simulations. WACCM+DART also reproduces the ozone variability that occurred during January and February 2009. The application of WACCM+DART to the 2009 SSW demonstrates the utility of WACCM+DART, and we anticipate WACCM+DART to be useful in future studies of short-term variability in the MLT. Last, we note that WACCM and DART are both community software packages, and the necessary software for the WACCM+DART data assimilation system is freely distributed through http://www.cesm.ucar.edu and http://www.image.ucar.edu/DAReS/DART/. We welcome, and encourage, other researchers to make use of WACCM+DART in the future.

Acknowledgments
SABER Version 2.0 available from http://saber.gats-inc.com is used in the present study. The Aura MLS observations are from the Goddard Earth Sciences Data and Information Services Center (http://disc.sci.gsfc.nasa.gov/Aura/).The lower atmosphere observations were obtained from NCEP Reanalysis Products (http://rda.ucar.edu/datasets/ds090.0/) and the COSMIC Data Analysis and Archive Center (http://cdaac-www.cosmic.ucar.edu/cdaac/index.html). WACCM and DART software is available from http://www.cesm.ucar.edu/ and http://www.image.ucar.edu/DAReS/DART/, respectively. The National Center for Atmospheric Research is sponsored by the National Science Foundation. This work was supported in part by a NCAR Advanced Study Program Postdoctoral Fellowship (N. Pedatella) and from NSF grant AGS-1138784 and NASA LWS grant NNX09AJ83G.

References

Alexander, M. J., et al. (2010), Recent developments in gravity-wave effects in climate models and the global distribution of gravity-wave momentum flux from observations and models, *Q. J. R. Meteorol. Soc.*, *136*, 1103–1124, doi:10.1002/qj.637.
Anderson, J. L. (2001), An ensemble adjustment Kalman filter for data assimilation, *Mon. Weather Rev.*, *129*, 2884–2903.
Anderson, J. L. (2009), Spatially and temporally varying adaptive covariance inflation for ensemble filters, *Tellus*, *61*, 72–83.

Anderson, J. L., T. Hoar, K. Raeder, H. Liu, N. Collins, R. Torn, and A. F. Arellano (2009), The data assimilation research testbed: A community data assimilation facility, *Bull. Am. Meteorol. Soc.*, *90*, 1283–1296, doi:10.1175/2009BAMS2618.1.

Chandran, A., R. R. Garcia, R. L. Collins, and L. C. Chang (2013), Secondary planetary waves in the middle and upper atmosphere following the stratospheric sudden warming event of January 2012, *Geophys. Res. Lett.*, *40*, 1861–1867, doi:10.1002/grl.50373.

Coy, L., S. Eckermann, and K. Hoppel (2009), Planetary wave breaking and tropospheric forcing as seen in the stratospheric sudden warming of 2006, *J. Atmos. Sci.*, *66*, 495–507.

Davis, R. N., J. Du, A. K. Smith, W. E. Ward, and N. J. Mitchell (2013), The diurnal and semidiurnal tides over Ascension Island (8°S, 14°W) and their interaction with the stratospheric QBO: Studies with meteor radar, eCMAM and WACCM, *Atmos. Chem. Phys. Discuss.*, *13*, 4785–4837, doi:10.5194/acpd-13-4785-2013.

Derber, J. C., and W.-S. Wu (1998), The use of TOVS cloud-cleared radiances in the NCEP SSI analysis system, *Mon. Weather Rev.*, *126*, 2287–2299.

Eckermann, S. D., et al. (2009), High-altitude data assimilation system experiments for the northern summer mesosphere season of 2007, *J. Atmos. Sol. Terr. Phys*, *71*, 531–551.

Funke, B., M. López-Puertas, D. Bermejo-Pantaleón, M. García-Comas, G. P. Stiller, T. von Clarmann, M. Kiefer, and A. Linden (2010), Evidence for dynamical coupling from the lower atmosphere to the thermosphere during a major stratospheric warming, *Geophys. Res. Lett.*, *37*, L13803, doi:10.1029/2010GL043619.

Garcia, R. R., D. R. Marsh, D. E. Kinnison, B. A. Boville, and F. Sassi (2007), Simulation of secular trends in the middle atmosphere, 1950-2003, *J. Geophys. Res.*, *112*, D09301, doi:10.1029/2006JD007485.

Gaspari, G., and S. Cohn (1999), Construction of correlation functions in two and three dimensions, *Q. J. R. Meteorol. Soc.*, *125*(554), 723–757.

Goncharenko, L. P., A. J. Coster, R. A. Plumb, and D. I. V. Domeisen (2012), The potential role of stratospheric ozone in the stratosphere-ionosphere coupling during stratospheric warnings, *Geophys. Res. Lett.*, *39*, L08101, doi:10.1029/2012GL051261.

Hoppel, K. W., N. L. Baker, L. Coy, S. D. Eckermann, J. P. McCormack, G. E. Nedoluha, and D. E. Siskind (2008), Assimilation of stratospheric and mesospheric temperatures from MLS and SABER into a global NWP model, *Atmos. Chem. Phys. Discuss.*, *8*, 8455–8490, doi:10.5194/acpd-8-8455-2008.

Hoppel, K. W., S. D. Eckermann, L. Coy, G. E. Nedoluha, D. R. Allen, S. D. Swadley, and N. L. Baker (2013), Evaluation of SSMIS upper atmosphere sounding channels for high-altitude data assimilation, *Mon. Weather Rev.*, *141*, 3314–3330, doi:10.1175/MWR-D-13-00003.1.

Jin, H., Y. Miyoshi, D. Pancheva, P. Mukhtarov, H. Fujiwara, and H. Shinagawa (2012), Response of migrating tides to the stratospheric sudden warming in 2009 and their effects on the ionosphere studied by a whole atmosphere-ionosphere model GAIA with COSMIC and TIMED/SABER observations, *J. Geophys. Res.*, *117*, A10323, doi:10.1029/2012JA017650.

Kalnay, E., et al. (1996), The NCEP/NCAR 40-year reanalysis project, *Bull. Am. Meteorol. Soc.*, *77*, 437–470.

Liu, H.-L., F. Sassi, and R. R. Garcia (2009), Error growth in a whole atmosphere climate model, *J. Atmos. Sci.*, *66*, 173–186.

Manney, G. L., M. J. Schwartz, K. Kruger, M. L. Santee, S. Pawson, J. N. Lee, W. H. Daffer, R. A. Fuller, and N. J. Livesey (2009), Aura Microwave Limb Sounder observations of dynamics and transport during the record-breaking 2009 Arctic stratospheric major warming, *Geophys. Res. Lett.*, *36*, L12815, doi:10.1029/2009GL038586.

Marsh, D. R., R. R. Garcia, D. E. Kinnison, B. A. Boville, F. Sassi, S. C. Solomon, and K. Matthes (2007), Modeling the whole atmosphere response to solar cycle changes in radiative and geomagnetic forcing, *J. Geophys. Res.*, *112*, D23306, doi:10.1029/2006JD008306.

Marsh, D. R., M. J. Mills, D. E. Kinnison, J.-F. Lamarque, N. Calvo, and L. Polvani (2013a), Climate change from 1850 to 2005 simulated in CESM1(WACCM), *J. Clim.*, *26*, 7372–7391, doi:10.1175/JCLI-D-12-00558.1.

Marsh, D. R., D. Janches, W. Feng, and J. M. C. Plane (2013b), A global model of meteoric sodium, *J. Geophys. Res. Atmos.*, *118*, 11,442–11,452, doi:10.1002/jgrd.50870.

McCormack, J. P., L. Coy, and K. W. Hoppel (2009), Evolution of the quasi 2-day wave during January 2006, *J. Geophys. Res.*, *114*, D20115, doi:10.1029/2009JD012239.

McLandress, C., J. F. Scinocca, T. G. Shepherd, M. C. Reader, and G. L. Manney (2013), Dynamical control of the mesosphere by orographic and nonorographic gravity wave drag during the extended northern winters of 2006 and 2009, *J. Atmos. Sci.*, *70*, 2152–2169, doi:10.1175/JAS-D-12-0297.1.

Neale, R. B., J. Richter, S. Park, P. H. Lauritzen, S. J. Vavrus, P. J. Rasch, and M. Zhang (2013), The mean climate of the Community Atmosphere Model (CAM4) in forced SST and fully coupled experiments, *J. Clim.*, *26*, 5150–5168, doi:10.1175/JCLI-D-12-00236.1.

Nezlin, Y., Y. J. Rochon, and S. Polavarapu (2009), Impact of tropospheric and stratospheric data assimilation on mesospheric prediction, *Tellus*, *61A*, 154–159.

Palo, S. E., R. G. Roble, and M. E. Hagan (1999), Middle atmosphere effects of the quasi-two-day wave determined from a general circulation model, *Earth, Planets Space*, *51*, 629–647.

Pedatella, N. M., H.-L. Liu, and M. E. Hagan (2012), Day-to-day migrating and nonmigrating tidal variability due to the six-day planetary wave, *J. Geophys. Res.*, *117*, A06301, doi:10.1029/2012JA017581.

Pedatella, N. M., K. Raeder, J. L. Anderson, and H.-L. Liu (2013), Application of data assimilation in the Whole Atmosphere Community Climate Model to the study of day-to-day variability in the middle and upper atmosphere, *Geophys. Res. Lett.*, *40*, 4469–4474, doi:10.1002/grl.50884.

Pedatella, N. M., et al. (2014), The neutral dynamics during the 2009 sudden stratosphere warming simulated by different whole atmosphere models, *J. Geophys. Res. Space Physics*, 1306–1324, doi:10.1002/2013JA019421.

Polavarapu, S. M., S. Ren, Y. Rochon, D. Sankey, N. Ek, J. Koshyk, and D. Tarasick (2005), Data assimilation with the Canadian Middle Atmosphere Model, *Atmos. Ocean*, *43*, 77–100.

Raeder, K., J. L. Anderson, N. Collins, T. J. Hoar, J. E. Kay, P. H. Lauritzen, and R. Pincus (2012), DART/CAM: An ensemble data assimilation system for CESM atmospheric models, *J. Clim.*, *25*, 6304–6317, doi:10.1175/JCLI-D-11-00395.1.

Randall, W. J. (1993), Global variations of zonal mean ozone during stratospheric warming events, *J. Atmos. Sci.*, *50*, 3308–3321.

Randall, C. E., V. L. Harvey, D. E. Siskind, J. France, P. F. Bernath, C. D. Boone, and K. A. Walker (2009), NOx descent in the Arctic middle atmosphere in early 2009, *Geophys. Res. Lett.*, *36*, L18811, doi:10.1029/2009GL039706.

Ren, S., S. Polavarapu, S. R. Beagley, Y. Nezlin, and Y. J. Rochon (2011), The impact of gravity wave drag on mesospheric analyses of the 2006 stratospheric major warming, *J. Geophys. Res.*, *116*, D19116, doi:10.1029/2011JD015943.

Richter, J. H., F. Sassi, and R. R. Garcia (2010), Towards a physically based gravity wave source parameterization in a general circulation model, *J. Atmos. Sci.*, *67*, 136–156.

Rong, P. P., J. M. Russell III, M. G. Mlynczak, E. E. Remsberg, B. T. Marshall, L. L. Gordley, and M. López-Puertas (2009), Validation of Thermosphere Ionosphere Mesosphere Energetics and Dynamics/Sounding of the Atmosphere using Broadband Emission Radiometry (TIMED/SABER) v1.07 ozone at 9.6 μm in altitude range 15-70 km, *J. Geophys. Res.*, *114*, D04306, doi:10.1029/2008JD010073.

Sankey, D., S. Ren, S. Polavarapu, Y. J. Rochon, Y. Nezlin, and S. Beagley (2007), Impact of data assimilation filtering methods on the mesosphere, *J. Geophys. Res.*, *112*, D24104, doi:10.1029/2007JD008885.

Sassi, F., H.-L. Liu, J. Ma, and R. R. Garcia (2013), The lower thermosphere during the northern Hemisphere winter of 2009: A modeling study using high-altitude data assimilation products in WACCM-X, *J. Geophys. Res. Atmos.*, *118*, 8954–8968, doi:10.1002/jgrd.50632.

Sathishkumar, S., and S. Sridharan (2013), Lunar and solar tidal variabilities in mesospheric winds and EEJ strength over Tirunelveli (8.7°N, 77.8°E) during the 2009 major stratospheric warming, *J. Geophys. Res. Space Physics*, *118*, 533–541, doi:10.1029/2012JA018236.

Schwartz, M. J., et al. (2008), Validation of the Aura Microwave Limb Sounder temperature and geopotential height measurements, *J. Geophys. Res.*, *113*, D15S11, doi:10.1029/2007JD008783.

Siskind, D. E., M. H. Stevens, M. Hervig, F. Sassi, K. Hoppel, C. R. Englert, and A. J. Kochenash (2011), Consequences of recent Southern Hemisphere winter variability on polar mesospheric clouds, *J. Atmos. Sol. Terr. Phys.*, *73*(13), 2013–2021.

Tunbridge, V. M., D. J. Sandford, and N. J. Mitchell (2011), Zonal wave numbers of the summertime 2 day planetary wave observed in the mesosphere by EOS Aura Microwave Limb Sounder, *J. Geophys. Res.*, *116*, D11103, doi:10.1029/2010JD014567.

Wang, H., T. J. Fuller-Rowell, R. A. Akmaev, M. Hu, D. T. Kleist, and M. D. Iredell (2011), First simulations with a whole atmosphere data assimilation and forecast system: The January 2009 major sudden stratospheric warming, *J. Geophys. Res.*, *116*, A12321, doi:10.1029/2011JA017081.

Yuan, T., C.-Y. She, D. A. Krueger, F. Sassi, R. Garcia, R. G. Roble, H.-L. Liu, and H. Schmidt (2008), Climatology of mesopause region temperature, zonal wind, and meridional wind over Fort Collins, Colorado (41°N, 105°W), and comparison with model simulations, *J. Geophys. Res.*, *113*, D03105, doi:10.1029/2007JD008697.

